

PHYSICAL REVIEW B

CONDENSED MATTER

THIRD SERIES, VOLUME 27, NUMBER 9

1 MAY 1983

Nuclear-quadrupole-resonance study of the ground state of praseodymium in lanthanum trifluoride

B. R. Reddy and L. E. Erickson

National Research Council, Ottawa, Ontario K1A 0R6, Canada

(Received 3 January 1983)

A nuclear-quadrupole-resonance study of trivalent praseodymium in a lanthanum trifluoride single crystal is presented. The magnitudes and orientation of the enhanced nuclear Zeeman tensor are obtained for the six magnetically inequivalent sites from measurements in 100-G magnetic fields. By comparing the directions of the site y axis and the crystal a axis, it is concluded that the Pr^{3+} site symmetry is C_2 and not C_s . From a study of the polarization of the optical pump transition for each Pr^{3+} site, it is determined that the ${}^3H_4(0\text{ cm}^{-1})\text{--}{}^1D_2(16\,872\text{ cm}^{-1})$ optical transition is an electric dipole transition.

INTRODUCTION

In a preliminary study,¹ some nuclear-quadrupole-resonance (NQR) measurements of the trivalent praseodymium-ion dilute in lanthanum fluoride single crystals were reported. In this paper, we give a complete study of the hyperfine structure of the ground 3H_4 state obtained by exhaustive magnetic-site-selective measurements of resonance frequencies as a function of the orientation of a 100-G magnetic field in relation to the crystal axes.

The $\text{LaF}_3:\text{Pr}^{3+}$ crystal has become a classic system. Many techniques, such as cw rf-optical double resonance,¹ photon echo²⁻⁴ and free-induction decay,⁵ and photon-echo-nuclear double resonance,^{6,7} have been used in its study. As a consequence, much is known about it. Crystal-field electronic eigenfunctions have been given by Matthies and Welsch.⁸ However, the results of this paper would suggest that a host crystal having a higher site symmetry and fewer magnetic sites should be used so that rigorous comparisons of the experiments with theory could be made.

The LaF_3 host crystal has been the subject of considerable controversy because different types of experiments lead to different conclusions concerning its structure. The crystal electric field, which completely lifts the otherwise degenerate multiplets, leads to an anisotropic nuclear Zeeman tensor for each crystallographic site. The sites are orientationally related by crystal symmetry operations. How many inequivalent magnetic impurity sites are

there? How are they oriented in relation to the crystal axes? Andersson and Proctor⁹ examined the La^{3+} NQR and concluded that there were six La^{3+} sites. Sharma,¹⁰ in an EPR study of Gd^{3+} in LaF_3 , found three. Baker and Rubins¹¹ in a study of Ce^{3+} , Nd^{3+} , Dy^{3+} , Er^{3+} , and Yb^{3+} in LaF_3 found six sites. Some doubt was raised that crystal twinning was responsible for the six-site conclusions and that in fact only three magnetically inequivalent sites existed in the crystal.¹² This was encouraged by the lack of agreement on the crystal space-group symmetry.¹³⁻¹⁶ This space-group ambiguity led to a controversy about the Pr^{3+} site symmetry.¹⁰ Is it D_{3h} , C_{2v} , C_2 , or C_s ? In this paper, we address the questions of the anisotropic Zeeman tensor, its orientation with respect to the crystal axes, number of Pr^{3+} sites, and Pr^{3+} site symmetry.

CRYSTAL STRUCTURE

The LaF_3 crystal structure has been studied by a number of investigators. A number of structures have been proposed, and with each structure a La site symmetry suggested. Oftedal¹³ concluded that the LaF_3 single crystal fitted the $P6_3/mcm$ (D_{6h}^3) space group with C_{2v} site symmetry. Schlyter¹⁴ proposed a $P6_3/mmc$ (D_{6h}^4)— D_{3h} description. Mansmann¹⁵ and Zalkin¹⁶ decided that the x-ray data are fitted best by the $P\bar{3}c1$ (D_{3d}^4) space group with C_2 site symmetry. The neutron diffraction measurements¹⁷ yield a $P6_3cm$ (C_{6v}^3)— C_s structure. The most relevant experiment to our NQR work is

that of Andersson and Proctor,⁹ and the addendum by Andersson and Johansson.¹² They concluded that the only La^{3+} site symmetry consistent with the NQR data was C_2 . If no distortion of the lattice takes place when Pr^{3+} substitutes for La^{3+} then the Pr^{3+} site symmetry must also be C_2 .

X-ray observations of our crystal were made using a single-crystal diffractometer.¹⁸ When the x-ray beam was incident on the center of the face along the [0001] direction, the x-ray scattering was consistent only with $P\bar{3}c1$ symmetry. Near the edges, some reflections due to the $P6_3/mmc$ structure were observed. Our NQR experiments were sensitive only to ions in the center of the crystal. We therefore should anticipate a C_2 site symmetry with three inequivalent magnetic sites per unit cell. These x-ray data, together with Laue patterns, were used to orient the crystal for the NQR experiments. The Laue pattern with the reciprocal-lattice axes for our crystal is shown in Fig. 1. The crystal axes are rotated by 30° away from the reciprocal-lattice axes.

ENERGY LEVELS AND HAMILTONIANS

The trivalent praseodymium ion has two equivalent ($4f$) electrons in addition to closed shells. The low-symmetry C_2 crystal electric field removes all degeneracy from the $(4f)^{2S+1}L_J$ multiplets. In the absence of a nuclear spin, all levels are singlets. Time-reversal symmetry requires that $\langle n | \vec{J} | n \rangle = 0$ for all levels $|n\rangle$ (in the absence of an external magnetic field), that is there is no net electronic magnetization. (In doubly degenerate states, this magnetization corresponds to a magnetic field at the nucleus of 1 MG interacting with the nuclear spin producing a hyperfine interaction of order 1 GHz.) The conven-

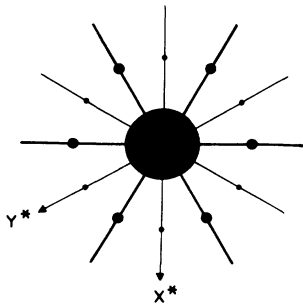


FIG. 1. Laue back-reflection pattern for $\text{LaF}_3:\text{Pr}^{3+}$. The reciprocal-lattice axes are shown on the diagram. The two a axes in real space are oriented $\pi/6$ away from x^* and y^* so that the local C_2 axes coincide with the intense reflections at "5 o'clock," "9 o'clock," etc.

tional Hamiltonian for such a system is given by

$$H = A_J \vec{J} \cdot \vec{I} + P [I_z^2 - \frac{1}{3} I(I+1)] + \frac{1}{3} P \eta (I_x^2 - I_y^2) + g \beta \vec{H} \cdot \vec{J} - g_N \beta_N \vec{H} \cdot \vec{I}, \quad (1)$$

where the first term is the magnetic hyperfine interaction, the second the nuclear quadrupole interaction, and the last two are the electron and nuclear Zeeman interactions. The nuclear spin I is $\frac{5}{2}$. Because all electronic levels are singlet, the first term produces no first-order hyperfine interaction. The Hamiltonian may be rewritten

$$H = -\hbar(\gamma_x H_x I_x + \gamma_y H_y I_y + \gamma_z H_z I_z) + D [I_z^2 - \frac{1}{3} I(I+1)] + E (I_x^2 - I_y^2) \quad (2)$$

as was given by Teplov¹⁹ where

$$\gamma_i / 2\pi \text{ (in kHz G}^{-1}\text{)} = (g_N \beta_N + 2g \beta \Lambda_{ii}) / h, \quad i = x, y, z \quad (3)$$

$$\Lambda_{ii} = \sum_{n \neq 0} \frac{A_j |\langle 0 | J_i | n \rangle|^2}{\epsilon_n - \epsilon_0}, \quad (4)$$

where ϵ_n is the energy of level n ,

$$D = D_a + P_{4f} + P_{\text{lat}}, \quad (5)$$

$$E = E_a + (P\eta/3)_{\text{lat}} + (P\eta/3)_{4f},$$

$$D_a = A_j [\frac{1}{2}(\Lambda_{xx} + \Lambda_{yy}) - \Lambda_{zz}], \quad (6)$$

$$E_a = A_j (\Lambda_{yy} - \Lambda_{xx}) / 2, \quad (7)$$

$$P_{4f} = -\frac{3e^2 Q}{4I(2I-1)} \langle r^{-3} \rangle_{4f} (1-R) \times \langle J || \alpha || J \rangle \langle |3J_z^2 - J(J+1)| \rangle, \quad (8)$$

$$\eta_{4f} = \frac{3 \langle |J_x^2 - J_y^2| \rangle}{\langle |3J_z^2 - J^2| \rangle},$$

$$P_{\text{lat}} = -\frac{3Q}{2I(2I-1)} \frac{B_{20}}{\langle r^2 \rangle} \frac{1-\gamma_\infty}{1-\sigma_2}, \quad (9)$$

$$\eta_{\text{lat}} = B_{22} / B_{20}.$$

Here, $B_{20} = 2A_{20} \langle r^2 \rangle$; $(1-\gamma_\infty)$, $(1-R)$, and $(1-\sigma_2)$, respectively, represent the Sternheimer factors for the lattice electric-field gradient, the mean inverse r cube, and the mean r square for the $4f$ electrons. A_j is the hyperfine constant for the given J state.

This assumes that all of the tensor quantities have the same axis system, which is not a symmetry requirement for C_2 site symmetry. It is necessary to rotate all tensor quantities into a common axis sys-

tem. This will be pursued in the discussion section. The hyperfine levels consist of three doubly degenerate levels for each electronic singlet in the absence of a magnetic field. The spacings are of order 10 MHz. In a magnetic field, the magnetic splitting factors are anisotropic because the second-order magnetic hyperfine interaction contributes an enhancement of the external magnetic field.¹⁹ This Hamiltonian is fitted to NQR frequency versus magnetic field direction data to obtain all of the parameters. Note, however, that the separation of the various contributions to D and E require more information than is obtained in these experiments.

EXPERIMENTS

The NQR measurements were made using a rf-optical double resonance technique described previously.¹ A $\text{LaF}_3:\text{Pr}^{3+}$ (0.05 at. %) single crystal, cooled to 5 K, was illuminated by a single-frequency dye laser beam to excite the ${}^3H_4(0\text{ cm}^{-1})\text{-}{}^1D_2(16\,872\text{ cm}^{-1})$ optical transition. Only one ground-state hyperfine level is resonant with the laser for a pumped ion. The hf state mixing due to the nonaxial symmetry of the quadrupole interaction gives a nonzero transition probability from the upper level back to both unpumped ground hyperfine levels. Because of the very slow spin-lattice relaxation (1 s compared to a fluorescence lifetime of 1 ms), excess population in the unpumped ground levels builds up after a few pumping cycles. The total fluorescence output from the crystal drops from its initial value by a factor of 10 in 100 ms as the population of the pumped hf level is transferred to other ground-state levels. (The inhomogeneously broadened optical line ensures all hyperfine levels are pumped by the laser.) This leads to large population redistributions in the ground state which are interrogated by an rf magnetic field. The NQR is detected when the rf magnetic field [approximately 0.1 G (rms)], resonant with a ground-state energy-level separation, induces magnetic dipole transitions tending to equalize the population, causing the fluorescence intensity to increase (by as much as a factor of 3).

The rf magnetic field is produced by a current in a single loop surrounding the sample. The current is obtained from a 10-W power amplifier driven by a computer-controlled frequency synthesizer. The 100-G static external magnetic field is obtained from a computer-controlled three-axis Helmholtz magnet previously described.²⁰ The magnetic field is rotatable in planes and cones through 4π geometry to an accuracy of 0.1 G and 0.3° . The fluorescence from the ${}^1D_2(16\,872\text{ cm}^{-1})$ level to the ${}^3H_4(195\text{ cm}^{-1})$ level is monitored with the aid of a 0.2-m spectrometer and C31034 photomultiplier us-

ing photon-counting techniques. Several scans of fluorescence versus frequency are averaged in a typical run.

RESULTS

A large number of scans of fluorescence versus frequency were made. These fell into two groups—those for the $I_z = \frac{1}{2} - \frac{3}{2}$ transitions in the vicinity of 8.5 MHz, and those for the $I_z = \frac{3}{2} - \frac{5}{2}$ transition near 16.7 MHz. The $I_z = \frac{1}{2} - \frac{1}{2}$ transition was not observed presumably because the fast $\frac{1}{2} - \frac{1}{2}$ relaxation kept the populations equal in spite of optical pumping. Typical scans are shown in Fig. 2. The magnetic field vector is at 45° from the crystal C_3 axis in a plane perpendicular to a crystal a axis. From

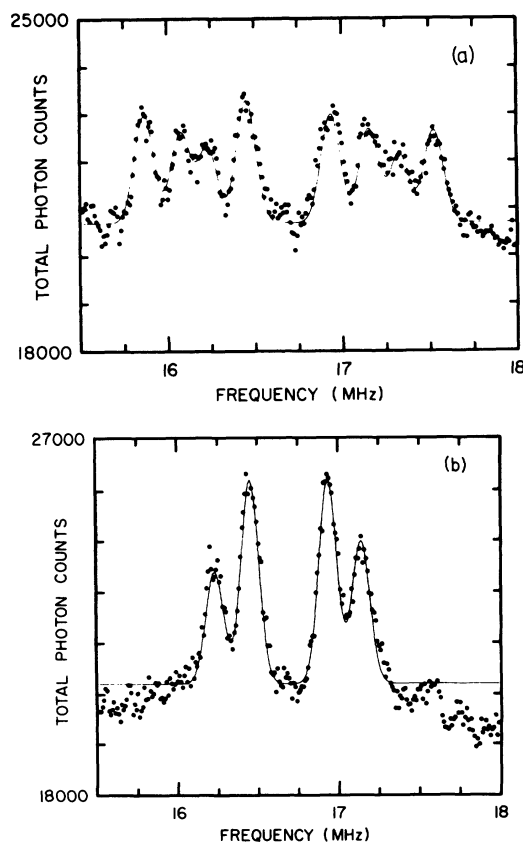


FIG. 2. Optically detected NQR in the ground electronic state of Pr^{3+} in LaF_3 host single crystal. ($I_z = \frac{3}{2} - \frac{5}{2}$ transition.) The 100-G magnetic field is in a plane containing C_3 and perpendicular to C_2 and is at an angle $\pi/4$ from C_3 . The lines on the far left and on the far right originate from a site whose z axis lies in that plane. (a) The exciting light is polarized along C_2 . (b) The exciting light is polarized perpendicular to C_2 and C_3 . Note the outer pair of lines is "turned off."

scans for many different directions of the magnetic field, it is possible to map the resonance frequencies versus field angle and determine the direction of the z axis of the nuclear Zeeman tensor. These maps are shown in Figs. 3–5 for the $I_z = \frac{3}{2} - \frac{5}{2}$ transitions for the magnetic field always in a plane. Six z axes are observed. In Fig. 4 where the field that is always in a plane containing the C_3 axis and perpendicular to the C_2 axis, the two outer solid curves show two sites with the local z axis at an angle of 81.4° relative to the C_3 axis. The inner curves show four sites which are degenerate in pairs, with the same angle of inclination relative to the C_3 axis. The six sites are related to one another by a $2\pi/3$ rotation about the C_3 axis and a reflection in a plane perpendicular to the C_3 axis. The z axes are not symmetry axes of the crystal.

The maps of the $I_z = \frac{1}{2} - \frac{3}{2}$ transition are much more complex because all three magnetic splitting factors are active. Maps of this transition are shown in Figs. 6 and 7. The data were fitted by the Hamiltonian equation (2) to yield the parameters given in Table I.²¹ The solid lines in Figs. 3–7 are the least-squares best-fit calculation of frequency versus field angle. These fits were made assuming that the axes of all tensor quantities were coincident.

The maximum NQR signal for a given magnetic site occurs when the E vector of the pump laser is perpendicular to the C_3 axis and parallel to the y axis of the site. The site y axis is parallel to an a axis of LaF_3 crystal. The optical transition is σ polarized (in relation to the crystal C_3 axis). It is possible to selectively “turn off” sites by choosing the pump light polarization. Such a demonstration is given in Fig. 2(a) (on) and Fig. 2(b) (off). The identi-

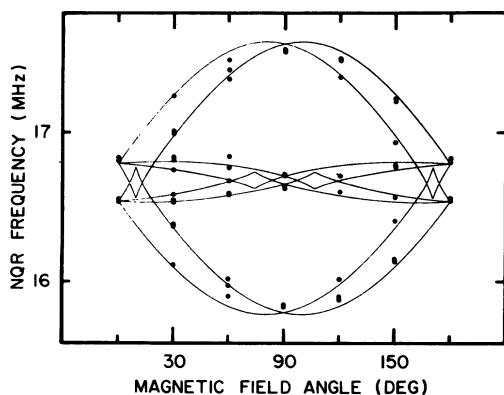


FIG. 3. NQR frequencies are mapped for the $I_z = \frac{3}{2} - \frac{5}{2}$ transition for the 100-G external magnetic field always in a plane containing C_2 and C_3 , as a function of field angle. 0° is along C_3 .

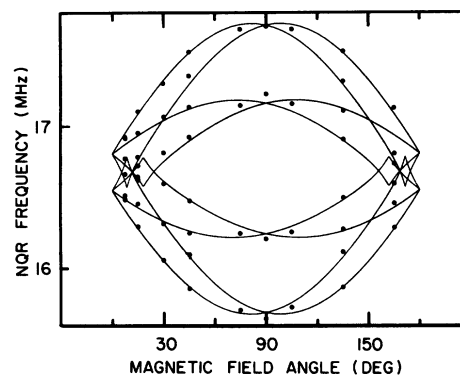


FIG. 4. NQR frequencies are mapped for the $I_z = \frac{3}{2} - \frac{5}{2}$ transition for the 100-G external magnetic field always in a plane perpendicular to C_2 , as a function of field angle. 0° is along C_3 .

ty of each NQR line was confirmed through comparing scans with differing optical polarizations. This magnetic site selection scheme was first reported by Shelby.²²

The magnetic-site-selection measurement shows that the optical pump transition is an electric dipole transition. (1) Figure 2 demonstrates that the maximum absorption for a given C_2 -symmetry site occurs when the light is polarized with the E vector parallel to the C_2 axis. (2) In a similar measurement, with the light along a C_2 axis (axial for that site), the axial site is not present, while the other two sites give strong signals.

The measurement of the angular dependence of the magnetic splitting factors provides sufficient data for a determination of the site symmetry of the

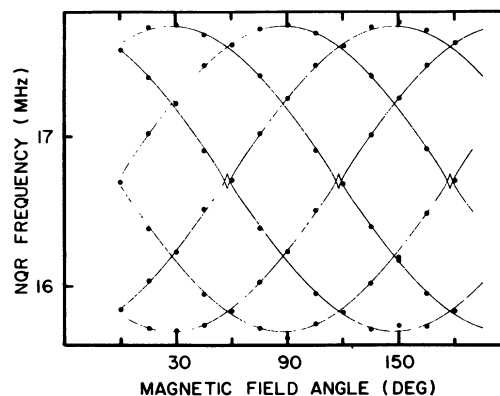


FIG. 5. NQR frequencies are mapped for the $I_z = \frac{3}{2} - \frac{5}{2}$ transition for the 100-G external magnetic field always in a plane perpendicular to C_3 , as a function of field angle. 0° is along C_2 .

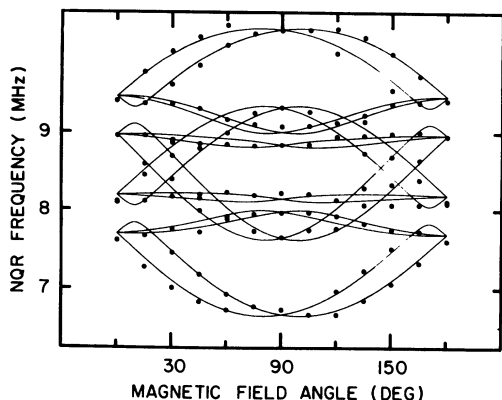


FIG. 6. NQR frequencies are mapped for the $I_z = \frac{1}{2} - \frac{3}{2}$ transition for the 100-G external magnetic field always in a plane containing C_3 and C_2 , as a function of field angle.

Pr^{3+} ion. The three Pr^{3+} y axes are perpendicular to the C_3 axis. If the site symmetry is C_s , the reflection plane must include the C_3 axis and a in order to transform the other a axes (and ligands) correctly. The symmetry-required common axis between the various tensor quantities for this low site symmetry is perpendicular to the reflection plane. If, however, the site symmetry is C_2 or C_{2v} , then the common axis is a . This common axis, either a or perpendicular to it, gives the site symmetry. We have shown that the common axis (y axis) is a for the magnetic splitting tensor; therefore the site symmetry is C_2 or C_{2v} . We have further shown that the z axis of the Pr^{3+} site does not lie along (or perpendicular to) a crystal symmetry axis, which is required for C_{2v} site symmetry. D_{3h} symmetry is excluded because the magnetic splitting tensor is not only nonaxial but also because C_3 is not the common axis. Now that

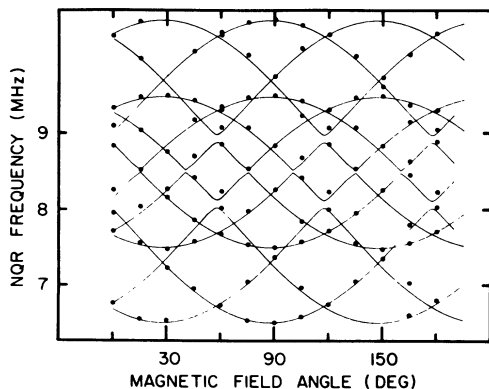


FIG. 7. NQR frequencies are mapped for the $I_z = \frac{1}{2} - \frac{3}{2}$ transition for the 100-G external magnetic field always in a plane perpendicular to C_3 , as a function of field angle.

TABLE I. Least-squares best-fit parameters for $\text{LaF}_3:\text{Pr}^{3+}$. The upper and lower bounds obtained by Chen *et al.* for each γ are given in parentheses. Λ_{ii} , D_a , and E_a are calculated from the experimental values of γ . The Λ_{ii} values in parentheses are calculated from Matthies and Welsch electronic wave functions and experimental energies considering only contributions from the 3H_4 levels. The experimental errors shown are the standard deviations of the parameters obtained from the least-squares fit.

$\gamma_x/2\pi = 4.98 \pm 0.04$ (−1.3; +8.3) kHz/G
$\gamma_y/2\pi = 2.53 \pm 0.03$ (−1.9; +7.7)
$\gamma_z/2\pi = 10.16 \pm 0.03$ (+7.1; +16.7)
$D = 4185 \pm 0.9$ kHz
$E = 146 \pm 0.9$ kHz
$\Lambda_{xx} = 1.64 \times 10^{-3}$ (1.92×10^{-3})
$\Lambda_{yy} = 5.49 \times 10^{-4}$ (2.01×10^{-3})
$\Lambda_{zz} = 3.96 \times 10^{-3}$ (2.56×10^{-3})
$D_a = 3132$ kHz
$E_a = 596$ kHz

the site symmetry is determined to be C_2 , a space group may be chosen from those proposed on the basis of the x-ray data. (The space group describes the positions of all of the ions in the crystal and gives the site symmetry for every position in the crystal.) For the $P6_3cm$ (C_{6v}^3) space group, the lanthanide ion lies on a reflection plane which contains a and C_3 . This yields C_s symmetry. For the $P\bar{3}C1$ (D_{3d}^4) space group, the lanthanide ion lies on a C_2 axis which contains a . This gives the observed C_2 symmetry. This space group is consistent with the x-ray measurements of our crystal. (At the edges of our crystal, the x-ray reflections gave the $P6_3/mmc$ space group, that is, a D_{3h} site symmetry. The NQR spectrum is not axial as would be required by such a high site symmetry.)

DISCUSSION

Chen *et al.*²³ published formulas for the range of γ_i to be expected in Pr^{3+} in a solid. These are given in Table I. All measured γ 's fall well within their predicted range. From the measured $\gamma_i/2\pi$ we may calculate Λ_{ii} , D_a , and E_a with the use of Eq. (4). The results are shown in Table I. Λ_{ii} were also calculated from the crystal-field (CF) wave functions of Matthies and Welsch. These are also included in Table I. The calculations would predict an almost isotropic $\gamma_i/2\pi$ and gives at least one value outside of Chen's limits.

The principal axis directions for the various tensor quantities are determined by the crystal electric

field. The quantities D and E are dominated by the second-order hyperfine interaction, which in turn are calculated from CF wave functions. All even B_{nm} terms to order 6 are required. The $4f$ electrons are shielded from the full impact of the crystal field.²⁴ The nuclear quadrupole moment also interacts with this crystal field, but now an antishielding factor $(1-\gamma_\infty)$ is the multiplier and only B_{nm} terms of order 2 are involved.²⁵ An estimate of the gradient may be obtained from the NQR measurements of La in LaF₃ (Refs. 9 and 26) where no ($4f$) electrons are present. (Since the Pr³⁺ ion is substituted for a La³⁺ ion, one would expect this field gradient at the nucleus to be the same for both ions with the exception of shielding due to the $4f$ electrons.) Finally, the two ($4f$) electrons produce a field gradient at the nucleus and give an interaction shielded by the closed shells by a factor $(1-R)$. The last two terms are much smaller than the first, so we shall ignore them.

The crystalline electric-field (CEF) z axis chosen by Matthies⁸ is common with the C_2 site axis, and his x axis is parallel to the C_3 axis of the crystal. From the EPR measurements,¹¹ one of the principal axis directions of the CEF tensor coincides with Matthies z axis, and the other axes are rotated by an angle α from C_3 . The nuclear rotation is about the C_2 site axis. Following Wokaun,²⁷ the $H_i(\gamma_i/2\pi)I_i$ term was transformed into the axis system of the CEF tensor. The solid lines of Figs. 3–7 were recalculated for a range of angles with no discernable im-

provement in the fit.

A rigorous comparison between theory and experiment will not be possible until a set of electronic eigenstates which give a more reasonable prediction for γ_i become available such as for LiYF₄:Pr³⁺.²⁸

CONCLUSIONS

The nuclear-quadrupole-resonance measurements of Pr³⁺ diluted in a LaF₃ single crystal show that six Pr³⁺ magnetically inequivalent sites of symmetry C_2 (and not C_3) are present. Six La³⁺ sites were observed by Andersson and Proctor in NQR measurements of the same crystal. However, the space group $P\bar{3}c1$, which gives the C_2 site symmetry and the observed x-ray reflections, accounts for only three. Andersson and Proctor suggested that microtwinning might be responsible for this discrepancy. Alternatively, the F-ion mobility observed by Lee and Sher²⁹ may yield several structures which are frozen at the temperatures of our experiments. The x-ray observations were at 293 K where mobility was observed. The measured anisotropic magnetic splitting factors $\gamma_i/2\pi$ disagree with those calculated using the crystal-field electronic wave functions of Matthies and Welsch. This discrepancy is due to wave functions which do not adequately describe the optical spectra. The optical pump transition, ³H₄-¹D₂(16 872 cm⁻¹), is shown to be an electric dipole transition.

¹L. E. Erickson, *Opt. Commun.* **21**, 147 (1977).

²N. Takeuchi and A. Szabo, *Phys. Lett.* **50A**, 361 (1974).

³Y. C. Chen and S. R. Hartmann, *Phys. Lett.* **58A**, 201 (1976).

⁴R. M. Macfarlane, R. M. Shelby, and R. L. Shoemaker, *Phys. Rev. Lett.* **43**, 1726 (1979).

⁵R. G. DeVoe, A. Szabo, S. C. Rand, and R. G. Brewer, *Phys. Rev. Lett.* **42**, 1560 (1979).

⁶K. Chiang, E. A. Whittaker, and S. R. Hartmann, *Phys. Rev. B* **23**, 6142 (1981).

⁷R. M. Macfarlane, C. S. Yannoni, and R. M. Shelby, *Opt. Commun.* **32**, 101 (1980).

⁸S. Matthies and D. Welsch, *Phys. Status Solidi B* **68**, 125 (1975).

⁹L. O. Andersson and W. G. Proctor, *Z. Kristallogr.* **127**, 366 (1968).

¹⁰V. K. Sharma, *J. Chem. Phys.* **54**, 496 (1971).

¹¹J. M. Baker and R. S. Rubins, *Proc. Phys. Soc. London* **78**, 1353 (1961).

¹²L. O. Andersson and G. Johansson, *Z. Kristallogr.* **127**, 386 (1968).

¹³I. Oftedal, *Z. Phys. Chem. Abt. B* **13**, 190 (1931).

¹⁴K. Schlyter, *Ark. Kemi* **5**, 73 (1952).

¹⁵M. Mansmann, *Z. Kristallogr.* **122**, 375 (1965).

¹⁶A. Zalkin, D. H. Templeton, and T. E. Hopkins, *Inorg. Chem.* **5**, 1466 (1966).

¹⁷C. de Rango, G. Tsoucaris and Ch. Zelwer, *C. R. Acad. Sci. C* **263**, 64 (1966).

¹⁸We thank Dr. Y. LePage of the Division of Chemistry, National Research Council of Canada, for making these measurements.

¹⁹M. A. Teplov, *Zh. Eksp. Teor. Fiz.* **53**, 1510 (1967) [*Sov. Phys.—JETP* **26**, 872 (1968)].

²⁰L. E. Erickson, *Rev. Sci. Instrum.* **51**, 1095 (1980).

²¹In a preliminary study (Ref. 1), $\gamma_2/2\pi$ was reported as 23 kHz/G. A factor of 2 was omitted in the data analysis. I thank K. K. Sharma for pointing this out.

²²R. M. Shelby and R. M. Macfarlane, *Opt. Commun.* **27**, 399 (1978).

²³Y. C. Chen, K. Chiang, and S. R. Hartmann, *Opt. Commun.* **22**, 181 (1979).

²⁴D. T. Edmonds, *Phys. Rev. Lett.* **10**, 129 (1963).

²⁵S. Hüfner, *Optical Spectra of Transparent Rare Earth Compounds* (Academic, New York, 1978), pp. 45 and

- 176.
- ²⁶Y. C. Chen, K. P. Chiang, and S. R. Hartmann, *Opt. Commun.* **26**, 269 (1978).
- ²⁷A. Wokaun, S. C. Rand, R. G. DeVoe, and R. G. Brewer, *Phys. Rev. B* **23**, 5733 (1981).
- ²⁸K. K. Sharma and L. E. Erickson, *J. Phys. C* **14**, 1329 (1981).
- ²⁹K. Lee and A. Sher, *Phys. Rev. Lett.* **14**, 1027 (1965).